



# Simulation and Experiment of Worm Gear Thermal Deformation and Transmission Error

Yong Zheng<sup>1,2</sup>, Hao Huang<sup>1</sup>, Yan Chen<sup>3</sup>, Donglin Peng<sup>1</sup> (✉), and Ziran Chen<sup>1,2</sup>

<sup>1</sup> Engineering Research Center of Mechanical Testing Technological and Equipment, Ministry of Education, Chongqing University of Technology, Chongqing 400054, China  
pd1@cqut.edu.cn

<sup>2</sup> Chongqing Key Laboratory of Time Grating Sensing and Advanced Testing Technology, Chongqing University of Technology, Chongqing 400054, China

<sup>3</sup> College of Electrical and Electronic Engineering, Chongqing University of Technology, Chongqing 400054, China

**Abstract.** With the wide application of worm gear drive in precision equipment, the requirements for its transmission accuracy are becoming higher and higher. Among many influencing factors, the influence of indoor temperature change on transmission accuracy can not be ignored, which needs to further analyze the transmission error of worm gear pair under different ambient temperatures. In order to study the influence of thermal deformation of worm gear pair on transmission accuracy, this paper theoretically calculates the geometric deformation of worm gear teeth after heating, and gives the polar coordinate expression of tooth profile after thermal deformation. The solid model of worm gear is established by SolidWorks, and the thermal structure analysis of finite element software is carried out to obtain the temperature distribution of worm gear after thermal deformation and the deformation of tooth profile geometry. Then the deformed worm gear is introduced into ADAMS for dynamic analysis, and the variation law of worm gear transmission error with temperature is obtained. Finally, it is verified by experiments.

**Keywords:** Worm gear · Ambient temperature · Thermal deformation · Transmission accuracy

## 1 Introduction

According to the existing research, the thermal error accounts for 40% of the total error of precision machine tools, and the transmission accuracy of worm gear and worm is an important factor affecting the machining accuracy of machine tools [4]. Therefore, the research on the thermal deformation of worm gear pair has important academic significance. Li yunqi and Zhang Ruiliang analyzed the temperature field of the tooth root of the cylindrical gear by using the finite element software, and finally obtained the variation law of the temperature and the tooth root stress of the gear [5]. Cheng Fuan and others combined the tribology and meshing principle of worm gear transmission. In order to obtain the geometric and kinematic characteristics of worm gear tooth surface,

© The Author(s) 2023

L. Yan and J. Na (Eds.): ICFPMCE 2022, AHE 10, pp. 333–346, 2023.

[https://doi.org/10.2991/978-94-6463-022-0\\_29](https://doi.org/10.2991/978-94-6463-022-0_29)

they established the mathematical model of worm gear steady-state temperature field, and studied the temperature field distribution of worm gear tooth surface through the calculation of input heat flux and convection coefficient [6].

At present, there are many researches on the thermal deformation of worm gear pair and gear pair, but most of them do not consider the influence of ambient temperature on the geometric dimension of worm gear pair. Generally, the temperature of the constant temperature workshop is about 20 °C, but the worm gear processed at 20 °C is used at other temperatures. Its transmission accuracy has changed, and errors will occur in the transmission process. In this paper, through the finite element simulation and dynamic simulation of the worm gear, the temperature field and transmission error of the worm gear pair under different ambient temperatures are analyzed and studied. Through the method of parametric design, the influence of temperature on the transmission accuracy of the worm gear pair is analyzed.

## 2 Thermal Deformation Principle of Worm Gear Pair

Deformation under heat is the basic property of materials. When many materials are heated, their size will change, and this deformation caused by temperature change is called thermal deformation. There are many factors to be considered in the calculation of thermal deformation, among which the key is the distribution of internal temperature and heat conduction. The distribution of temperature is the main factor causing the thermal deformation of parts, because the deformation occurs with the change of temperature. Secondly, the thermal expansion performance of materials can not be ignored [7]. If different thermal expansion coefficients of materials are selected, the thermal deformation of parts will be different under the same temperature conditions, that is, the errors will be different.

### 2.1 Thermal Deformation Analysis of Worm Gear

Because the instantaneous surface temperature of the meshing tooth surface changes in the process of worm gear transmission. However, the influence range of instantaneous surface temperature is limited to a very thin layer of thermal surface, so it is generally assumed that the temperature of each point on the worm gear is a fixed value. In addition, the meshing time of each tooth of the worm gear in one cycle of worm gear rotation is shorter, which is much shorter than the time required for the change of worm gear temperature distribution. Therefore, it can be assumed that the temperature distribution of each tooth is the same and a constant value is maintained.

When the temperature changes, the height and thickness of the worm gear teeth will be deformed, resulting in the points on the worm gear tooth profile deviate from the original position, as shown in Fig. 1.

Then the polar coordinate parameter equation of the actual tooth profile after thermal deformation is:

$$\begin{cases} r_{k2} = r_k + \Delta r_k = \frac{r_b + u_b \cos \alpha_k + \Delta t \lambda r_b (1 - \cos \alpha_k)}{\cos \alpha_k} \\ \theta_{k2} = \theta_k - \Delta \theta_k = \text{inv} \alpha_k - \frac{\Delta t \lambda S_k}{2r_{k2}} \end{cases} \quad (1)$$

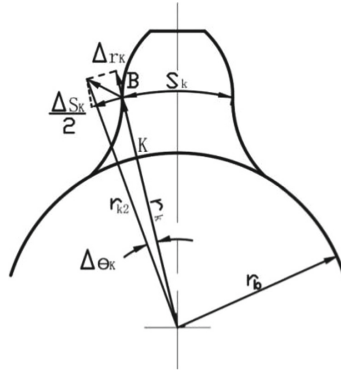


**Fig. 1.** The position of tooth profile point after thermal deformation.

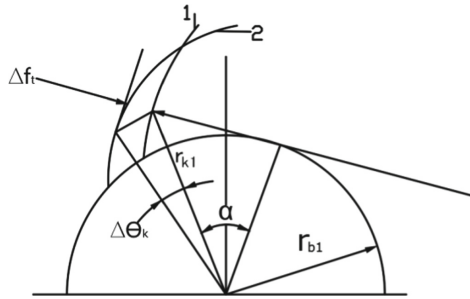


**Fig. 2.** The tooth profile error of worm gear caused by temperature change.

where,  $r_{k2}$  is the polar diameter on the actual contour after thermal deformation, is the polar diameter on the theoretical contour,  $r_k$  is the polar diameter variation,  $\Delta r_k$  is the radius of the base circle,  $r_b$  is the thermal deformation of the base circle,  $u_b$  is the pressure angle at any point on the involute of the base circle,  $\alpha_k$  is the temperature variation,  $\lambda$  is the linear expansion coefficient of the material,  $\theta_2$ ,  $\theta_k$  is the expansion angle, and  $\Delta\theta$  is the expansion angle.

It can be seen from the above formula that the theoretical pressure angle is different from the pressure angle after deformation, so the polar diameter and extension angle have changed. This shows that after the thermal deformation of the worm gear, the points on the actual tooth profile are no longer satisfied with the equation of the theoretical involute, that is, the temperature change has an impact on the tooth profile of the worm gear, and brings the tooth profile error, which affects the accuracy of the worm gear transmission.

In order to explain the deviation degree between the actual tooth profile and the theoretical involute tooth profile of the worm gear after thermal deformation, a thermal deformation error is introduced, that is, the normal distance between the actual thermal deformation tooth profile and the theoretical involute tooth profile in the working part of the worm gear tooth height. As shown in Fig. 2.

In Fig. 2, 1 represents the theoretical tooth profile and 2 represents the actual tooth profile. Therefore, without considering the influence of other factors on the worm gear, the tooth profile error caused by temperature change is:

$$\begin{aligned} \Delta f_t &= \Delta \theta_k r_{k1} \cos \alpha = -\frac{\Delta t \lambda}{2(1 + \Delta t \lambda)} \left[ \frac{s}{r} - \right. \\ &\quad \left. 2(\operatorname{inv} \alpha_k - \operatorname{inv} \alpha)(1 + \Delta t \lambda) r_b \right] \quad (2) \\ &= \Delta t \lambda r_b \operatorname{inv} \alpha_k - \frac{\Delta t \lambda r_b}{2} \left( \frac{s}{r} + 2 \operatorname{inv} \alpha \right) \end{aligned}$$

In the formula,  $\Delta f$  is the tooth profile error of the worm gear,  $r_{k1}$  is the polar diameter of the base circle after thermal deformation,  $\alpha$  is the pressure angle,  $S$  is the tooth thickness of the indexing circle, and  $r$  is the radius of the indexing circle.

### 2.2 Analysis of Worm Thermal Deformation

The worm will deform axially and radially after heating, but the thermal deformation in the axial direction is the main factor affecting the accuracy of worm gear and worm transmission. Therefore, this paper mainly studies the thermal deformation in the axial direction of the worm. Because one end of the worm is relatively fixed, when it is heated, it will produce an expansion to the free end along the axis direction. The influence of this expansion is to make the worm move towards the free end at its meshing position [8–10]. The expansion at the same temperature is directly proportional to the length of the material, that is, the worm gear; The expansion of meshing tooth surface is different, which has a great impact on the transmission accuracy of worm gear.

The coefficient of linear expansion of the material is that the elongation of the material with a length of 1 m is the coefficient of linear expansion for each rise of 1. Then the formula for calculating the thermal expansion of the worm is as follows:

$$\alpha_{\text{expansion}} = \Delta t \alpha_{\text{material}} \frac{l}{100} \quad (3)$$

In the formula,  $\alpha_{\text{expansion}}$  is the actual expansion of the worm,  $\Delta t$  is the change of temperature,  $\alpha_{\text{material}}$  is the inherent differential accuracy of the material, and the major influence is the thermal deformation in the axial direction.  $l$  is the equivalent length of the worm.

### 3 Transmission Error Analysis of Worm Gear Pair

Transmission error  $t_e$  refers to the difference between the actual motion and the theoretical motion in the transmission process. When the actual motion output value of the output end is different from the theoretical output value, it will cause transmission error. This kind of error will lead to vibration and noise in the transmission process [11]. In serious cases, it will also cause manufacturing error and shape error of workpieces. Therefore, transmission error has always been a problem of great concern in the industrial field.

Because the worm gear has geometric deformation after heating, it can be seen from formula (3) above that the deformation of the worm in the axial direction is greater than

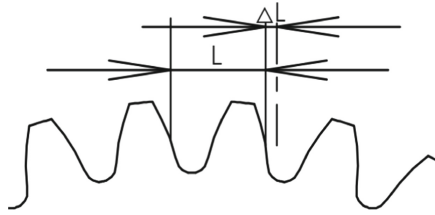


Fig. 3. Rotation distance of worm gear after thermal deformation.

that of the worm gear in the radial direction, that is, when the worm rotates one turn, the worm gear rotates more in the horizontal direction than before the thermal deformation, resulting in transmission error. The rotation distance of the worm gear after the worm turns one circle after thermal deformation is shown in Fig. 3.

Since the workpiece is often processed at the low-speed end, when calculating the worm gear and worm transmission error, the angular displacement of the worm at the high-speed end is often converted (divided by the transmission ratio  $I$ ) to the worm gear at the low-speed end for comparison, and the transmission error of the worm gear and worm is:

$$TE_i = \frac{\Phi_{1i}}{I} - \Phi_{2i} \tag{4}$$

In the formula,  $TE_i$  is the transmission error value of point  $i$ ,  $I$  is the transmission ratio of worm gear,  $\Phi_{2i}$  is the angle value of worm gear at point  $i$ , and  $\Phi_{1i}$  is the angle value of worm at point  $i$ .

Because the errors calculated by the above formula are discrete points, it can be understood as the transmission error of single measurement, and then after summing them, the transmission error is:

$$TE = \sum \Delta TE_k = \sum \left( \frac{\Phi_{1k}}{I} - \Phi_{2k} \right) \tag{5}$$

In the formula,  $\Delta TE_k$  is the transmission error measured in a single time,  $\Phi_{1k}$  is the angle value of the worm at point  $k$ , and  $\Phi_{2k}$  is the angle value of the worm gear at point  $k$ .

### 4 Thermal Structural Simulation of Worm Gear

The finite element simulation software ANSYS is used for thermal simulation analysis of worm gear pair, and then the simulation result data is extracted. ADAMS is used to simulate the movement of worm gear pair, and the simulation results are extracted and then plotted.

Firstly, determine the materials and material properties selected by the worm gear, because different materials will affect its thermal expansion coefficient [12], and the simulation results will be different. The material properties of the worm gear are shown in Table 1.

**Table 1.** Properties of materials

Name	Material	Coefficient of expansion/(m/°C)	Modulus of elasticity /GPa	Poisson's ratio
Worm gear	ZCuSn10P1	$16.7 \times 10^{-6}$	115	0.34
Worm	40Cr	$12.5 \times 10^{-6}$	210	0.3

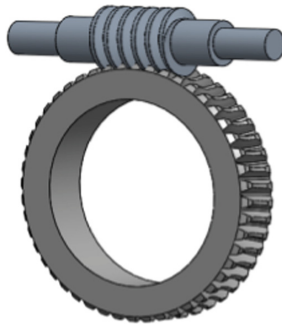


**Fig. 4.** Finite element model of worm gear.



**Fig. 5.** Model after meshing.

Import the worm gear model into ANSYS, as shown in Fig. 4. When doing ANSYS simulation, the worm gear will automatically generate contact pairs at its meshing points, and can mesh as needed. Because the tooth surface of worm gear is an irregular spatial curved surface, especially the tooth of worm gear, its shape is very complex, so the free mesh method is selected for finite element mesh division. Considering the number of grids and the solving speed, the unit size is set to 2 mm. The number of divided nodes is 35,991,357, and the number of units is 26,392,654. Figure 5 shows the model after meshing of worm gear.

Through the analysis of the boundary value conditions of the temperature field, combined with the actual situation of the worm gear, it is finally decided to take the change of the ambient temperature as the main factor affecting the geometric accuracy [13]. Therefore, the first type of boundary condition is selected, that is, the instantaneous temperature of any point on the object surface is known, then:

$$T_S = f(t) \quad (6)$$

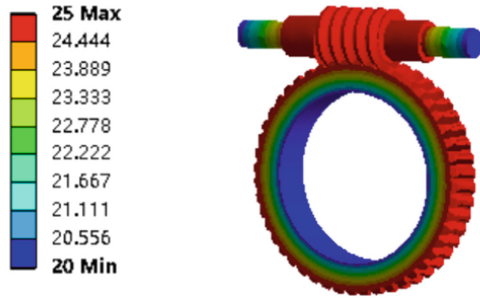
where,  $T_S$  is the surface temperature of the object. If the surface temperature remains unchanged,  $T_S$  is a constant.

Because this paper only considers the influence of ambient temperature on the worm gear, the constraint mode is set: add frictionless constraint to the inner circle of the worm gear, and apply cylindrical constraint to the bearing fit at both ends of the worm.

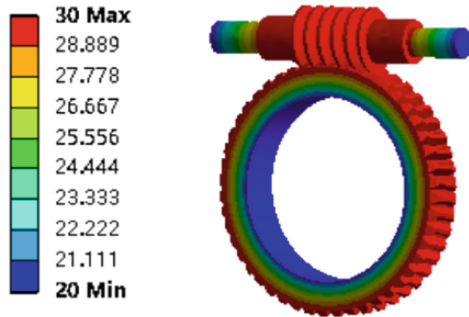
Because the worm gear working in our laboratory is in the range of 25 °C to 35 °C for a long time, the worm gear pair is studied based on the actual ambient temperature in the laboratory. Set the variation range of ambient temperature as 25 °C to 35 °C. The initial condition of analysis is that the worm gear is at 20 °C, and the temperature load of 25 °C, 30 °C, 35 °C is applied to the surface in contact with the environment, The obtained temperature field distribution is shown in Fig. 6.

It can be clearly seen from Fig. 6 that the outer ring temperature of the worm gear is high and concentrated. The temperature decreases gradually along the radial direction to the inner ring. This is because the outer ring of the worm gear is in contact with the environment, the inner ring is connected with the machine, and the heat is transferred from the outer ring to the inner ring. Therefore, the temperature is also lower as it goes inward along the axial direction. The change of overall dimension of worm gear caused by temperature change is shown in Fig. 7.

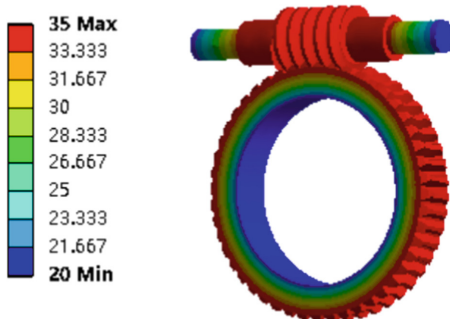
It can be clearly seen from Fig. 7 that with the increase of ambient temperature, the deformation of the worm gear is changing, the deformation of the worm gear gradually increases from the inner ring to the outer ring, and the maximum deformation is obtained at the outermost ring. The deformation of the worm increases gradually from bottom to top, and the maximum deformation is at the top of the worm. This shows that when the ambient temperature changes, the maximum deformation of the worm gear is at the position of tooth width or tooth height. However, in the post-processing module, click the displacement view command to accurately know the thermal changes of the worm



(a) Temperature distribution of worm gear at 25°C.



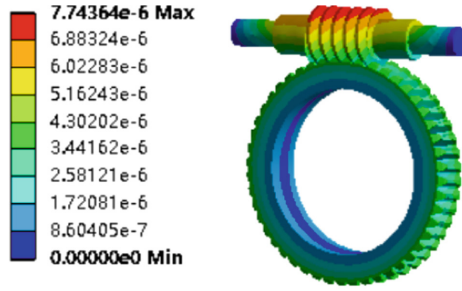
(b) Temperature distribution of worm gear at 30°C.



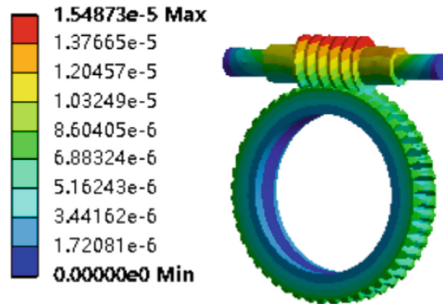
(c) Temperature distribution of worm gear at 35°C.

**Fig. 6.** Temperature distribution of worm gear at different temperatures.

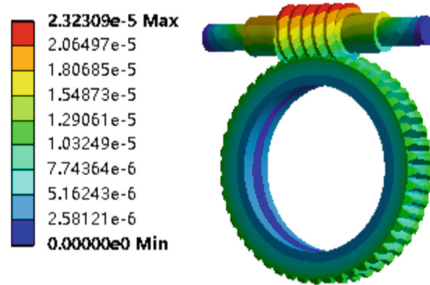
gear pair in the axial and tangential directions at the meshing, that is, the deformation of the tooth height and width of the worm gear. The relationship between temperature and the thermal deformation of worm gear tooth width and tooth height is shown in Fig. 8 and Fig. 9.



(a) Thermal deformation of worm gear at 25°C.



(b) Thermal deformation of worm gear at 30°C.



(c) Thermal deformation of worm gear at 35°C.

**Fig. 7.** Thermal deformation of worm gear at different temperatures.

The simulation results show that with the increase of ambient temperature, the thermal deformation of tooth width and tooth height of worm gear are also increasing. It can be seen from Fig. 8 and Fig. 9 that the curve of the thermal deformation of the worm gear tooth width and tooth height has an upward trend, which clearly shows that the change of ambient temperature has a certain impact on the tooth shape size of the worm gear, and the deformation of the worm is greater at the same temperature.

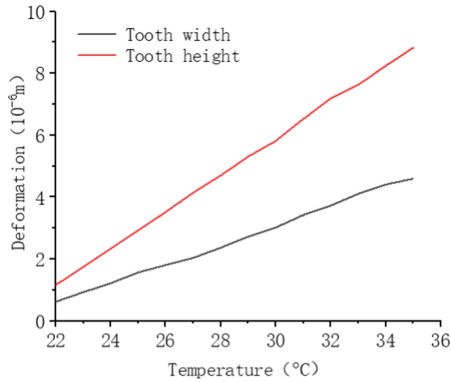


Fig. 8. Thermal deformation of worm gear.

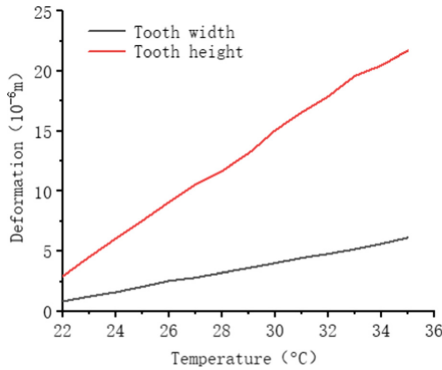


Fig. 9. Worm thermal deformation.

### 5 Worm Gear Motion Simulation and Experiment

Firstly, the three-dimensional model of worm gear established by SolidWorks is imported into ADAMS. As shown in Fig. 10.

Then determine the material properties of the worm gear as shown in Table 1, and then add contact constraints at the engagement of the worm gear, add rotating pairs on the worm gear, add rotating pairs and drive pairs on the worm [14]. The model of virtual prototype is shown in Fig. 11.

Set the speed of the worm as 48(°)/s. Since the transmission ratio of the worm gear is 48, the speed of the worm gear can be calculated as 1(°)/s. Set the simulation time to 360 s, so as to ensure that the worm gear rotates once, and more intuitively see the relationship between the rotation angles of the worm gear and worm. The rotation angle curve of the worm gear and worm obtained by simulation is shown in Fig. 12.

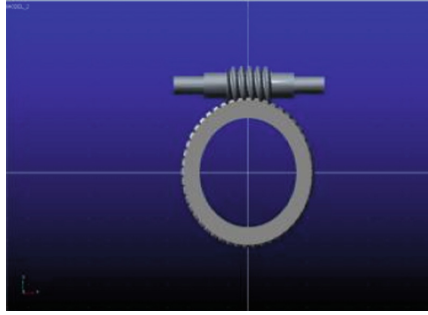


**Fig. 10.** Three dimensional model of worm gear.

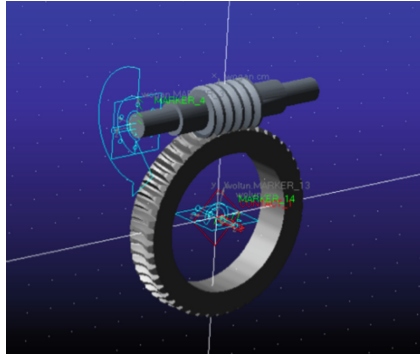


**Fig. 11.** Virtual prototype model.

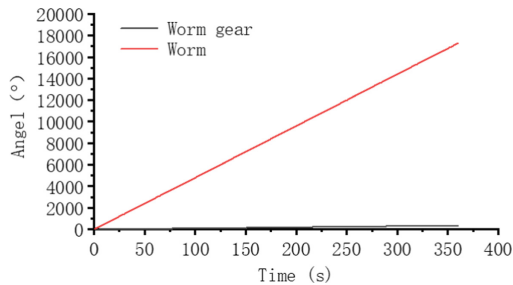


**Fig. 12.** Rotation angle of worm gear.

It can be seen from Fig. 12 that the rotation curves of the worm gear and the worm are straight lines inclined upward, and the ratio of the two is about 48. Because the sizes of the worm gear and worm are the original sizes, the transmission at this time can be regarded as the transmission of the worm gear under 20 °C, and Fig. 12 is the transmission relationship before the thermal deformation of the worm gear and worm. After processing the data, the transmission error of worm gear can be obtained, as shown in Fig. 13.

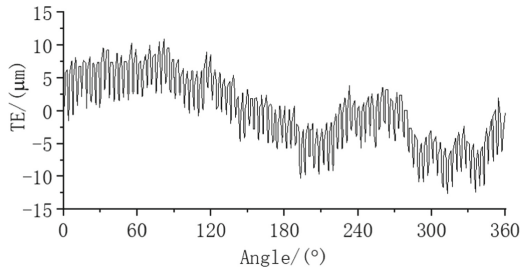


**Fig. 13.** Worm gear transmission error before thermal deformation.

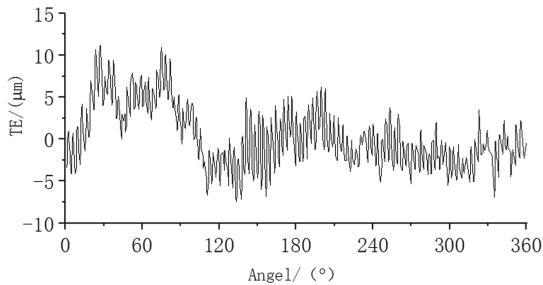


**Fig. 14.** Worm gear transmission error after thermal deformation.

Similarly, the worm gear after thermal deformation is imported into ADAMS. Here, the dimensions of worm gear, worm tooth width and tooth height are mainly changed. From the above worm gear thermal structure simulation results, it can be obtained that when 35 °C is, the worm gear tooth height and tooth width increase by 4.6 μm and 9.8 μm, while the worm tooth height and tooth width increase by 2.1 μm and 6.2 μm. After ADAMS motion simulation, the transmission error of worm gear after thermal deformation is finally obtained, as shown in Fig. 14.

The simulation results show that the transmission accuracy, i.e. transmission error, of the worm gear changes with the increase of the ambient temperature. It can be seen from Fig. 13 and Fig. 14 that the transmission error of the worm gear after thermal deformation fluctuates more than that before thermal deformation, and the image tends to move downward, but the peak value of the transmission error after thermal deformation is obviously larger than that before thermal deformation, Therefore, when the ambient temperature increases, the transmission error of worm gear and worm tends to become larger.

The theory is verified by the single-sided and double-sided meshing tester of GEARTEC and infrared thermal imager. The experimental site is shown in Fig. 15.

The experimental results show that when the worm gear pair temperature is 25 °C, the maximum transmission error is 26.8 μm, and when the worm gear pair temperature is 35 °C, the maximum transmission error is 27.5 μm. Therefore, it is concluded that with the increase of temperature, the transmission error of worm gear pair also increases, which is consistent with the previous simulation conclusion.

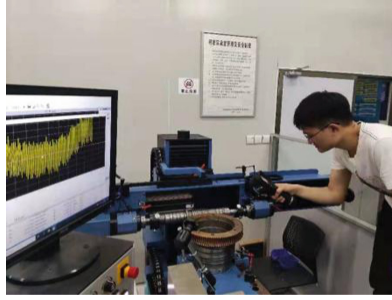


**Fig. 15.** Experimental site.

## 6 Conclusion

The thermal structural simulation of the worm gear is carried out by using the finite element software, and the thermal deformation of the tooth size of the worm gear under the condition of temperature change is obtained. Through ADAMS motion simulation software, the motion simulation of worm gear and worm is carried out to obtain the transmission error of worm gear and worm, and then through experimental verification, the influence relationship of temperature change on worm gear and worm transmission error is finally obtained, which provides an important reference and basis for controlling and reducing the thermal deformation of worm gear and worm and improving the transmission accuracy.

The analysis of this paper provides a basis for the high-precision analysis of worm gear and worm drive on the transmission error caused by thermal deformation. With the further research, the parameters of the transmission error change model caused by thermal deformation can be refined. With this model, the change of transmission error can be compensated by temperature information.

**Acknowledgments.** This work is supported by the National Major Scientific Research Instrument Development Project of China (Grant No. 51827805), Science and Technology, Research Program of Chongqing Municipal Education Commission (Grant No. KJQN202001150), Science and Technology Special Funds of Banan District of Chongqing (Grant No. 2020TJZ023), and the Science and Technology Research Program of Chongqing Municipal Education Commission (Grant KJZD-K201901105).

**Authors' Contributions.** Conceptualization, Yong Zheng and Donglin Peng; methodology, Yan Chen; software, Ziran Chen; formal analysis, Hao Huang; investigation, Yong Zheng; resources, Yong Zheng; data curation, Yong Zheng; writing—original draft preparation, Yong Zheng; writing—review and editing, Yong Zheng; visualization, Yong Zheng; supervision, Yong Zheng; project administration, Yong Zheng; funding acquisition, Yong Zheng. All authors have read and agreed to the published version of the manuscript.

## References

1. Zhang, Y.J., Xu, Y., Ma, X.Y., et al.: Research progress of worm gear materials in worm drive. *Mech. Drive* **44**, 170–176 (2020). <https://doi.org/10.16578/j.issn.1004.2539.2020.04.027>

2. Shi, X., Wang, W., Mu, Y., Yang, X.: Thermal characteristics testing and thermal error modeling on a worm gear grinding machine considering cutting fluid thermal effect. *Int. J. Adv. Manuf. Technol.* **103**(9–12), 4317–4329 (2019). <https://doi.org/10.1007/s00170-019-03650-0>
3. Litvin, F.L., Argentieri, G., De Donno, M.: Computerized design, generation and simulation of meshing and contact of face worm-gear drives. *Comput. Methods Appl. Mech. Eng.* **189**, 785–801 (2000). [https://doi.org/10.1016/S0045-7825\(99\)00329-1](https://doi.org/10.1016/S0045-7825(99)00329-1)
4. Dudas, L.: Modeling and simulation of a new worm gear drive having point-like contact. *Eng. Comput.* **29**, 251–272 (2013). <https://doi.org/10.1007/s00366-012-0271-0>
5. Li, Y.Q., Zhang, R.L., Wang, T., et al.: Analysis of the influence of temperature on the stress distribution of gear root. *Mech. Des. Manuf.* (6), 24–27 (2020). <https://doi.org/10.19356/j.cnki.1001-3997.2020.06.007>
6. Cheng, F., Jiao, J., Shi, J., et al.: Intelligent prediction system of worm gear transient temperature field based on artificial neural network. *J. Tianjin Univ.* **33**, 167–171 (2000). <https://doi.org/10.3969/j.issn.0493-2137.2000.02.009>
7. Li, G.H., Fei, Y.T.: Effect of temperature change on tooth profile of cylindrical gear. *Mech. Des.* **22**, 22–23 (2005). <https://doi.org/10.13841/j.cnki.jxsj.2005.02.008>
8. Chen, H.F., Wang, H., Zhai, P.P.: Thermodynamic analysis of worm gear based on finite element method. *Mech. Transm.* **38**, 170–172 (2014). <https://doi.org/10.16578/j.issn.1004.2539.2014.10.020>
9. Wang, S.L., Yang, Y., Li, X.G., et al.: Research on thermal deformation of large-scale computer numerical control gear hobbing machines. *J. Mech. Sci. Technol.* **27**, 1393–1405 (2013). <https://doi.org/10.1007/s12206-013-0320-7>
10. Yang, H.B., Li, G.Y., Li, J., et al.: Modeling and dynamic transmission error simulation analysis of ZA type worm pair. *Mech. Des. Manuf.* (9), 125–128 (2021)
11. Li, G.H., Fei, Y.T.: Study on non involute characteristics of standard involute gear during thermal deformation. *J. Harbin Inst. Technol.* **1**, 123–125 (2006)
12. Yang, H.F., Zhang, L.: Temperature field analysis of mechanical components of gear measuring machine based on ANSYS. *Mech. Electron.* **3**, 66–68 (2015)
13. Feng, A., Jing, G.F.: Study on the influence of temperature rise on the back clearance and indexing accuracy of worm gear pair. *Mech. Strength* **42**, 937–940 (2020)
14. Wang, F., Chen, J., Hong, R.J.: Simulation of worm gear transmission accuracy of tk13250e NC turntable based on ADAMS. *Mech. Transm.* **44**, 155–159 (2020). <https://doi.org/10.16578/j.issn.1004.2539.2020.03>

**Open Access** This chapter is licensed under the terms of the Creative Commons Attribution-NonCommercial 4.0 International License (<http://creativecommons.org/licenses/by-nc/4.0/>), which permits any noncommercial use, sharing, adaptation, distribution and reproduction in any medium or format, as long as you give appropriate credit to the original author(s) and the source, provide a link to the Creative Commons license and indicate if changes were made.

The images or other third party material in this chapter are included in the chapter's Creative Commons license, unless indicated otherwise in a credit line to the material. If material is not included in the chapter's Creative Commons license and your intended use is not permitted by statutory regulation or exceeds the permitted use, you will need to obtain permission directly from the copyright holder.

